International Conference "Water, Environment, Energy and Society" (WEES–2009)
New Delhi, 12–16 January 2009

Three Dimensional River Basin Simulation with Distributed Runoff Model for Water Quantity and Quality

Toshiharu Kojiri[1] and Amin Ismael Amin Nawahda
Water Resources Research Center
Disaster Prevention Research Institute,
Kyoto University, Gokasho, Uji, Kyoto 611-0011, JAPAN
E-mail: [1]tkojiri@wrcs.dpri.kyoto-u.ac.jp

ABSTRACT: Most of the existing distributed rainfall-runoff models simplify the interaction between the atmosphere and the groundwater processes. The objective of this research is to make an integrated hydrological model through the simulation of the hydrological interactions in the surface, ground and atmosphere. The methodology is based on the dynamic linking among the transient hydrological models at different time scales, which implies that the quantity and quality of the distributed runoff at every time step is affected by the impact of atmosphere and groundwater interactions.

INTRODUCTION

The distributed rainfall-runoff modeling was introduced in order to overcome the shortcomings of the traditional lumped models (Kojiri *et al.*, 2000). In this distributed modeling, the watershed is divided into two types of grids; terrain grids that have only excess precipitation as input, and river grids having both excess precipitation and river flow as input. The surface runoff in each grid is transformed into the corresponding next terrain or river grid. Each grid includes five land use types; mountain, paddy, agriculture, urban, and water body. At each grid the heat balance method is used to calculate the evaporation and snowmelt, and then the kinematic wave model is used for calculating the surface runoff. The linear storage model is used for groundwater flow modeling. The ground subsurface of the whole basin is divided into four uniform layers.

Most of the water quality studies consider the mineralization of degraded pollutants without considering the transformation products, even though those products can be more toxic, more soluble, more persistent, or more bio-accumulated than the parent compound. Therefore a reliable understanding of the chemical fate of pollutants is required for the environmental impact assessment.

The objective of this research is to make an integrated hydrological model through the simulation of the hydrological interactions in the surface, ground and atmosphere. The methodology is based on the dynamic linking among the transient hydrological models at different time scales, which implies that the quantity and quality of the distributed runoff at every time step is affected by the impact of atmosphere and groundwater interactions. Static linking of hydrological sub-models is normally used in distributed rainfall-runoff models. It is shown that the assumption of steady conditions for groundwater model during small time scales will not affect the accuracy of the model outputs. Using integrated hydrological modeling with dynamic linking between different sub-hydrological models is useful for water resources management.

COMPONENTS OF THE DISTRIBUTED HYDROLOGICAL RUNOFF MODEL

Evapotranspiration

For the distributed hydrological model, the actual evapotranspiration should be constructed. However the spatial and temporal meteorological data is usually not sufficiently dense. Recent researches for evapotranspiration simulation have not progressed enough to describe the spatial hourly variability of evapotranspiration. When simulating the evapotranspiration from a watershed with various land-uses and soil types the hourly time scale is of special importance.

The energy budget equation can be written for each grid in the watershed, as follows,

$$Q_o = Q_s - Q_r + Q_a - Q_{ar} - Q_{bs} - Q_e - Q_{lh} - Q_h - Q_g \quad \ldots (1)$$

where Q_o is the change in the grid energy; Q_s is the incident solar radiation; Q_r is the reflected solar radiation; Q_a is the incoming long wave atmospheric

radiation; Q_{ar} is the long wave radiation emitted by the grid; Q_{bs} is the long wave radiation emitted by the water body; Q_e is the energy used in evaporation; Q_{lh} is latent heat; Q_h is the sensible heat; and Q_g is the ground heat flux. The effective solar radiation intensity at the watershed has a spatial and temporal variation, given by,

$$I_o = \frac{W_o}{\left(1+0.017\cos\left[\frac{2\pi}{365}(186-D)\right]\right)^2}\sin\alpha \quad \ldots (2)$$

where I_o is the insolation, W_o is the solar constant, D is the Julian day, and α is the angle between the plan tangent to the earth and the projection of the solar radiation, sin α is donated by the solar altitude, given by,

$$\sin\alpha = \sin\delta\sin\Phi + \cos\delta\cos\Phi\cos\tau \quad \ldots (3)$$

where δ is the declination of the sun, Φ is the latitude, and τ is the hour angle, δ is approximated for a Julian day D, or

$$\delta = \frac{23.45\pi}{180}\cos\left[\frac{2\pi}{365}(172-D)\right] \quad \ldots (4)$$

The high temperature of the sun causes the shortwave radiation; the shortwave radiation can be estimated as reported by Curtis and Eagleson (1982), as

$$\frac{I_c}{I_o} = \exp(-na_1 m) \quad \ldots (5)$$

where n is the turbidity factor for air, it has the value of 2.0 for clear air to 5.0 for smoggy air, m is the optical air mass, and a_1 is defined as a function of the effective thickness of the atmosphere,

$$a_1 = 0.128 - 0.054\log_{10} m \quad \ldots (6)$$

m is estimated by the following equation,

$$m = \left[\sin\alpha + \frac{0.1500}{(\alpha+3.885)^{1.253}}\right]^{-1} \quad \ldots (7)$$

The cloud type, thickness, and elevation affect the shortwave radiation and an empirical equation in order to account this effect is formulated as follows,

$$\frac{I_s}{I_c} = 1-0.65N^2 \quad \ldots (8)$$

$$I_{sg} = K_t I_s \quad \ldots (9)$$

where K_t is the transmission coefficient function of density, type, and condition of buildings and vegetations, I_s is the net shortwave radiation, and N is total opaque could cover. The effective incoming shortwave radiation is given as follows,

$$I_s^* = I_s(1-albedo(t)) \quad \ldots (10)$$

Effective incoming shortwave radiation on snow surface is given by,

$$\frac{I_s}{I_s^*} = \exp(-kz) \quad \ldots (11)$$

where k is a function of snow pack density, and z is the depth of the snow pack. The values of K_t vary from 0.28 to 0.106 according to snowpack density (26%–45%). The earth surface, vegetations, and buildings are heated by the shortwave radiation from the sun, and then cause a longwave radiation as follows,

$$I_l = (1-albedo(t))\sigma E_a T_a^4 - \sigma E T^4 \quad \ldots (12)$$

where E_a is the atmosphere emissivity, σ is the Stefan-Boltzmann coefficient, T is the surface temperature, T_a is the air temperature (°C), and E is the atmosphere emissivity near the surface. E_a is related strongly to the vapor pressure e (hPa), which can be measured directly or calculated using the relative humidity measurements, (Idso, 1981),

$$E_a = 0.70 + 5.95\times10^{-5} e\times\exp\left(\frac{1500}{T_a}\right) \quad \ldots (13)$$

Over the snow pack E_a is taken as a constant and equal to 0.757. The energy transferred due to sensible heat can be estimated as follows,

$$Q_h = c_p\rho_a C_H U(T-T_a) \quad \ldots (14)$$

where C_H is the bulk transfer coefficient for sensible heat, c_p is the specific heat of air, ρ_a is the density of air (kg/m^3), and U is the wind speed (m/sec) measured at (2 m) above the ground surface, however wind speed is measured most commonly at (10 m) above the ground surface. The density of air is given by,

$$\rho_a = \frac{P_a}{RT_a}\left(1-0.378\frac{e}{P_a}\right) \quad \ldots (15)$$

where P_a is the atmosphere pressure (P_a). The temperature of the ground is affected by meteorological, terrain, and subsurface conditions. The meteorological conditions include net solar radiation, air temperature, and precipitation. Snow is considered as one of the important factors that affect the ground temperature. Also the distributed characteristics of the land uses and soil types affect the thermal coefficients of heat transfer such as the volumetric heat capacity, thermal conductivity, and the thermal diffusivity. If the ground has constant thermal proprieties, the fluctuation of ground temperature is approximated by Crawford *et al.* (1957),

$$T(z,t) = T'' + A_d \exp\left(-z\sqrt{\frac{\pi}{\alpha' t_o}}\right)\cos\left(\frac{2\pi t}{t_o} - z\sqrt{\frac{\pi}{\alpha' t_o}}\right) \quad \ldots (16)$$

where T'' is the ground seasonal average temperature, A_d is the difference between the maximum and minimum temperatures for the period, t is the time, to is time for one complete cycle, and ά is thermal diffusivity. The ground temperature decreases exponentially with depth. Many studies showed that the ground temperature below 5 meters is constant. The temperature elapse rate is around 1 degree per 50 m depth. The heat flow in the vertical direction is given by Baker (2000),

$$\frac{\partial T}{\partial t} = D_T \frac{\partial^2 T}{\partial z^2} \quad \ldots (17)$$

where D_T is the thermal diffusivity. The ground thermal conductivity is strongly affected by the water content. An empirical equation is used to describe the relation with soil moisture is given by Jansson (1991),

$$\lambda = A_\lambda + B_\lambda - (A_\lambda - D_\lambda)\exp\left(-(C_\lambda \theta)^4\right)$$

$$A_\lambda = \frac{(0.5 + 1.73\theta + 0.93S)}{(1 - 0.74\theta - 0.49M - 2.8S)} \quad \ldots (18)$$

$$B_\lambda = 2.8S \quad D_\lambda = 0.03 + 0.7S^2 \quad C_\lambda = 1 + 2.6\sqrt{MT}$$

where θ is the soil moisture. The variables S, M, and MT are percentages of solids, quartz, and clay in soil respectively. The latent heat is evaluated by the bulk-transfer method as follows,

$$Q_l = l\rho_a C_E U(q_s - q_a) \quad \ldots (19)$$

where l is the latent heat of vaporization, C_E is the bulk-transfer coefficient, q_s is the specific humidity at the water and atmosphere contact, q_a is the specific humidity of atmosphere.

The ground heat flow is estimated by using the soil temperature gradients measured near the surface with the one dimensional steady-conductive heat flow equation, or

$$Q_g = \lambda \frac{dT}{dz} \quad \ldots (20)$$

The change rate of the stored energy in the system during small time step is assumed constant. Evapotranspiration is the summation of evaporated and transpired water from water bodies and vegetations, the evapotranspiration is strangely affected by the soil moisture conditions, and also it is affected by the cropping type and stage. In this study evapotranspiration from each grid is evaluated by two steps, at first the evapotranspiration amount is calculated by using the FAO (1998) proposed crop factorization,

$$ET_1(grid,t) = k_f(type,t)\,EP(grid) \quad \ldots (21)$$

where k_f is the crop factor, type is the crop type, and E_P is the potential evaporation. At second the output of the first step is updated according to the mass balance equation in the subsurface model,

$$ET_2(\text{grid,t}) = \text{eprecipitation} + \text{irrigation} + \text{unsaturated/moisture} + \text{saturated/moisture} - EP - \text{recharge} - \text{runoff} \quad \ldots (22)$$

Surface Runoff

In this dissertation the surface runoff is simulated according to the kinematic wave model. It is based on the continuity and the kinematic assumptions,

$$\frac{\partial A}{\partial t} + \frac{\partial Q}{\partial s} = q(t,s) \quad \ldots (23)$$

$$A = f(x,Q) = \alpha Q^\beta \quad \ldots (24)$$

where A is the discharge area, Q is the flow rate, q is the spatial and temporal effective rainfall, and α and β are parameters. The Manning's equation is used to estimate the kinematic wave parameters,

$$Q = \frac{\sqrt{sin(\varphi)}}{n_r} A H^{\frac{2}{3}} \quad \ldots (25)$$

where φ is the grid average slope, nr is the roughness coefficient, and H is the hydraulic radius.

Groundwater Flow

Richards's equation for unsaturated flow in one dimension (Richards, 1931) is used to simulate the distribution of the soil moisture and to estimate the spatial and temporal groundwater recharge,

$$C\frac{\partial \Psi}{\partial t} = \frac{\partial}{\partial z}\left[K(\Psi)\left(\frac{\partial \Psi}{\partial z} + 1\right)\right] \quad \ldots (26)$$

where, C is the specific water capacity, ψ (m) is the water potential head, K is the hydraulic conductivity (m/sec), z (m) is the vertical coordinate and t is time. The potential pressure-saturation relation is simulated using van-Genuchten style equations,

$$S_t = \frac{\theta - \theta_r}{\theta_s - \theta_r} = \left[\frac{1}{1 + (\Psi/\Psi_d)^\alpha}\right]^{\lambda/\alpha} \quad \ldots (27)$$

$$K = K_s S_t^\eta \quad \ldots (28)$$

where S_t is the effective saturation, θ_r is the residual water content, θ_s is the saturated water content, α and λ are the van-Genuchten fitting parameters, Ψ_d is the displacement pressure head, K_s is the saturated

hydraulic conductivity and η is the exponential soil parameter.

Quasi-three dimensional differential equation for the transient unconfined groundwater flow with Dupuit assumptions is given by,

$$\frac{1}{2}\left(K_x \frac{\partial^2 h^2}{\partial x^2} + K_y \frac{\partial^2 h^2}{\partial y^2}\right) = S\frac{\partial h}{\partial t} - R(t) \qquad \ldots (29)$$

where h is the groundwater level, K is the hydraulic conductivity, S is the specific yield, R is the volume of recharge per unit time per unit aquifer area, x and y are the displacement coordinates, and t is time.

HYDROLOGICAL CHARACTERISTICS OF APPLIED CATCHMENT

Applied Catchment

The applied catchment, The Yasu River, is located in Shiga prefecture, Japan, and is one of the main water sources for Lake Biwa. Averaged annual precipitation for the regions ranges from 1550–2050 mm for the lower and upper catchments, respectively. The area of the whole basin is 445 km^2. The length of the river channel is 95 km. HydroBeam has been implemented mathematically and physically at a high resolution (1 km) land data, which involves several categories such as: land uses, soil types, topography, and geology, numerical simulations, and visualization tools, the watershed is divided into identical grids. In the Yasu River basin the stations used are Tsuchiyama, Minakuchi, Koka, Mikumo, Gamo and Yasu. This section briefly describes the differences in climate between these stations. Figure 1 shows the locations on the map.

Hydrological Characteristics of River Basin

In eight directions routing approach, flow from a grid is directed towards one of its eight neighbors with the steepest slope. HydroBEAM assigns a flow direction to each grid and a calculation index that represents the accumulated area down slope along the flow paths connecting each catchment's grids. However, the use of eight directions routing method has certain drawbacks in complex topographies as it permits flow only in one direction away from a DEM grid. Land use data is coupled with the soil characteristics for each grid in HydroBEAM in order to estimate the surface roughness that affects the velocity of runoff, and to estimate infiltration of precipitation. Leaf area index is estimated from the land use data. Land uses in data from seventy groundwater monitor wells were analyzed. For groundwater modeling the geological cross sections are analyzed, the soil and the geological maps are used in order to distribute the soil types and geological formations for each grid. There are five main soil types: (a) grey low land soil; (b) gray soil; (c) peat soil; (d) not matured soil; (e) dry brown forest soil.

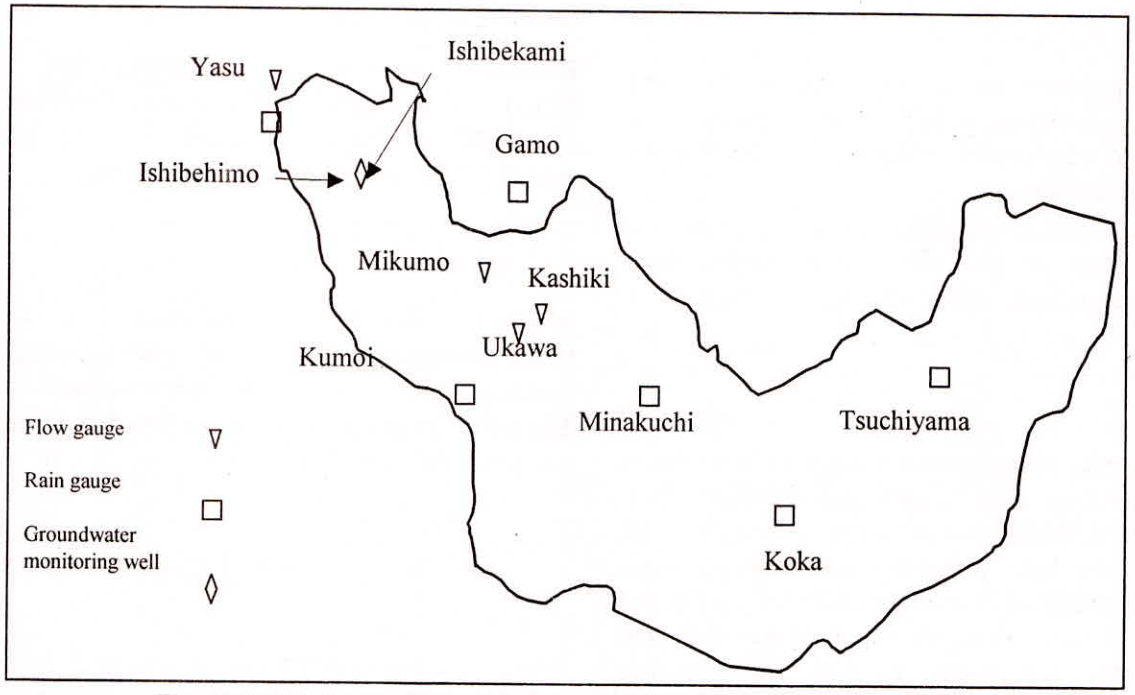

Fig. 1: Distributed weather and gauging stations at the Yasu River basin

Spatial and Temporal Variability of Hydrological Parameters

The surface and subsurface hydrological parameters vary in space and/or time; this variability causes a significant change in the shape of the river hydrograph. The variability can be caused by the basin characteristics, precipitation, and human utilization of land. Therefore, the watershed is divided into the catchments, each catchment is divided into square grids, and each grid is connected to a drainage network represented by a channel segment. The variability of the hydrological parameters for each grid is integrated, and then each grid is divided into elements of uniform parameters. The number of elements is decided by the surface properties and availability of hydrological data.

METEOROLOGICAL FORMULATION OF THE ATMOSPHERE

Distribution of Temperature

The spatial and temporal vertical temperature, pressure, and wind filed in each grid are calculated. And then the calculated data at an altitude of (2 m) is to be used in the heat budget relationship. Also the output data at a point source height is used for simulating the plume rise according to Gaussian plume model. The atmosphere is heated from each grid. The amount of solar energy received by a grid depends on time of day, seasonality, latitude, altitude and dynamic behaviors of land. The horizontal distribution of temperature is widely varied. Usually the vertical ambient temperature is reasonable assumed to be linear, and the vertical profile of temperature is calculated by using the lapse rate; it is usually varies between 5 and 8°C/km,

$$T_{i,j} = T^{*}_{i,j} - \Gamma.\Delta z \qquad \ldots (30)$$

where $T_{i,j}$ is the horizontal ambient temperature, $T^{*}_{i,j}$ is the measured ambient temperature, Γ is the lapse rate, and Δz is the change of altitude above the ground surface. In order to select the best lapse rate value for the distributing horizontal and vertical temperatures at the Yasu River basin. Temperature data form meteorological stations was analyzed in order to identify the correlation coefficient (R^2) among the weather stations.

Distribution of Air Pressure

The distribution of air pressure is obtained by assuming that the atmosphere layers are in hydrostatic condition and considered as an ideal gas. The distribution of the vertical and horizontal air pressures at a grid is derived as follows,

$$dp_{i,j} = -\rho g dz \quad \rho = \frac{RT_{i,j}}{P_{i,j}}$$

$$dP_{i,j} = -\frac{P_{i,j}}{RT_{i,j}} g dz \quad dz = -\frac{dT_{i,j}}{\Gamma}$$

$$\frac{dP_{i,j}}{P_{i,j}} = \frac{g}{R\Gamma}\frac{dT_{i,j}}{T} \quad P_{i,j} = P^{*}_{i,j}\left[\frac{T_{i,j}}{T^{*}_{i,j}}\right]^{\frac{g}{R\Gamma}} \qquad \ldots (31)$$

where P is the spatial and temporal air pressure, T is the spatial and temporal ambient temperature, * refers to measured values, i is the grid number, j is the time step, R is the dry air gas constant, and g is the gravitational acceleration. The derivation of Eqn. (31) is based on the assumption of constant lapse rate, however the use of a seasonal lapse rate is more reliable, which was shown in the previous section, but it doesn't affect much the related daily simulation of hydrological processes.

Distributed Wind Field

In the case of a distributed hydrological model, wind velocity is observed at randomly spaced meteorological stations within the watershed, and then an interpolation scheme is applied in order to estimate the wind field at each grid. This technique is based on averaging the wind velocities from distributed meteorological stations. Wind field is needed for calculating of the turbulent flux terms in the heat budget equation, and for calculating the concentration of air pollutants, C, in the equation of diffusion,

$$\frac{\partial C}{\partial t} + u\frac{\partial C}{\partial x} + \upsilon\frac{\partial C}{\partial y} + w\frac{\partial C}{\partial z} = K_x\frac{\partial^2 C}{\partial x^2} + K_y\frac{\partial^2 C}{\partial y^2} + K_z\frac{\partial^2 C}{\partial z^2} \qquad \ldots (32)$$

where u, v, and w are the components of the wind velocity, K is the diffusion coefficient. The solution can be approximated by using the Gaussian plume model if the Cartesian coordinate is replaced by new coordinate that is defined in terms of the wind velocity vector as follows,

$$\xi = \frac{\Phi(x,y)}{\sqrt{u^2+\upsilon^2}}, \qquad \eta = \frac{\Psi(x,y)}{\sqrt{u^2+\upsilon^2}} \qquad \ldots (33)$$

where Φ is the potential velocity, and Ψ is the stream function. Substituting of Eqn. (33) into the homogenous and the two dimensional form of Eqn. (32) gives,

$$\sqrt{u^2+\upsilon^2}\frac{\partial C}{\partial \xi}=K\left(\frac{\partial^2 C}{\partial \xi^2}+\frac{\partial^2 C}{\partial \eta^2}\right) \quad \ldots (34)$$

According to Gaussian plume model the solution is given by,

$$C(\xi,\eta)=\frac{Q}{\pi\sigma_\eta\sigma_z}\exp\left(-\frac{\eta^2}{2\sigma_\eta^2}-\frac{H^2}{2\sigma_z^2}\right) \quad \ldots (35)$$

where Q is the emission rate from a point source, and H is the effective height of a point source. The continuity equation can be applied in order to eliminate the divergence between successive grids as given by (Hiroh *et al.*, 1992),

$$\frac{\partial h}{\partial t}+\frac{\partial (uh)}{\partial x}+\frac{\partial (vh)}{\partial y}=0 \quad \ldots (36)$$

where h is the inversion height, u and v are the horizontal components of the wind velocity. The steady state is solved numerically by an iterative method. At a grid point (i, j), the finite difference approximation is given by,

$$D_{i,j}^n=\frac{\left(u_{i+1,j}^n h_{i+1,j}-u_{i-1,j}^n h_{i-1,j}\right)}{2\Delta x}+\frac{\left(\upsilon_{i,j+1}^n h_{i,j+1}-\upsilon_{i,j-1}^n h_{i,j-1}\right)}{2\Delta y} \quad \ldots (37)$$

where D is the divergence of the wind field, and n is the nth iteration. The velocity adjustments U and V,

$$\begin{aligned}
u_{i+1,j}^{n+1}&=u_{i+1,j}^n+s_{i+1,j}U_{i+1,j}^n h_{i+1,j}\\
u_{i-1,j}^{n+1}&=u_{i-1,j}^n+s_{i-1,j}U_{i-1,j}^n h_{i-1,j}\\
u_{i,j+1}^{n+1}&=u_{i-1,j}^n+s_{i,j+1}U_{i,j+1}^n h_{i,j+1}\\
u_{i,j-1}^{n+1}&=u_{i,j-1}^n+s_{i,j-1}U_{i,j-1}^n h_{i,j-1}
\end{aligned} \quad \ldots (38)$$

where s has a value of zero except for a grid, where there is no weather station, and a unity for other grids. Substitution of Eqn. (38) into Eqn. (37) yields,

$$\frac{\left(s_{i+1,j}+s_{i-1,j}\right)U_{i,j}^n}{2\Delta x}+\frac{\left(s_{i,j+1}+s_{i,j-1}\right)V_{i,j}^n}{2\Delta y}+D_{i,j}^n=0 \quad \ldots (39)$$

The two terms in Eqn. (39) are assumed to contribute equally to the divergence,

$$\begin{aligned}
U_{i,j}^n&=-D_{i,j}^n\left(\frac{\Delta x}{s_{i+1,j}+s_{i-1,j}}\right)\\
V_{i,j}^n&=-D_{i,j}^n\left(\frac{\Delta y}{s_{i,j+1}+s_{i,j-1}}\right)
\end{aligned} \quad \ldots (40)$$

The initial values of wind velocity in each grid, u_0 and v_0, are approximated using an empirical interpolation equation,

$$u_{i,j}^0=\frac{\sum_k u_k/r_k^2}{\sum_k 1/r_k^2},\qquad \upsilon_{i,j}^0=\frac{\sum_k \upsilon_k/r_k^2}{\sum_k 1/r_k^2} \quad \ldots (41)$$

Then, wind field is generated by using the approach that is based on the developed distributed pressures at each grid. The boundary and initial conditions in this approach are not only evaluated from the measured wind velocity from distributed weather stations, but also from large-scale output data from other atmosphere models. The output from the meso-scale model has a spatial resolution of 20 km and a time step of 6 hours. Then wind velocity is calculated by using the distribution of horizontal pressure gradients and then routed within the boundaries of the watershed. The wind flows from a higher pressure-grid to the least pressure-grid from the nearest neighboring grids as shown in Figure 2.

The distributed wind vectors are substituted in Eqn. (37) and modified by using the Eqn. (38) to Eqn. (40). In order to overcome the drawbacks of the distributed pressure-based method, the Ekman boundary layer can be used in order to approximate the wind vector profile at each grid based on a data-driven approach, and by considering the physical characteristics of the atmosphere near the surface of the ground. The wind field is simulated at every time step within the distributed hydrological model. The wind velocity, which is observed at the ground level, is distributed in the vertical direction by using the Ekman boundary layer approach, which is based on the balance among coriolis, pressure gradient and frictional forces, within the transition layer that ranges from 100 m to several kilometers or more, Pielke (1984). Above the surface layer the mean wind changes direction with height and approaches the free-stream velocity, geostrophic wind, at the top of the transition layer.

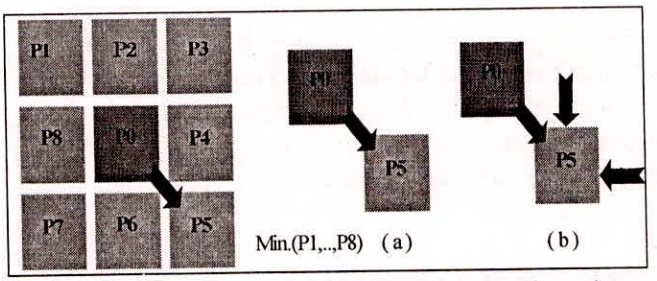

Fig. 2: Wind velocity routing algorithm; (a) 8-dierections based routing, (b) the case of sink-grid

The mass balance equation can be rewritten as,

$$0=\frac{1}{\rho_0}\frac{\partial}{\partial z}\rho_0\overline{w'u'}-\alpha_0\frac{\partial P_0}{\partial x}+fv \quad 0=\frac{1}{\rho_0}\frac{\partial}{\partial z}\rho_0\overline{w'v'}-\alpha_0\frac{\partial P_0}{\partial y}+fu \quad \ldots (42)$$

where f is the coriolis force. The subgrid flux terms are approximated with a constant exchange coefficient K_E. And then Eqn. (42) can be written in terms of the geostrophic wind components, v_g and u_g,

$$0 = K_E\frac{\partial^2 u}{\partial z^2}+f(v-v_g)$$

$$0 = K_E\frac{\partial^2 v}{\partial z^2}+f(u_g-u) \quad \ldots (43)$$

The geostrophic wind components are given by,

$$f\upsilon_g=\frac{1}{\rho_g}\frac{\partial P_g}{\partial x}, \qquad fu_g=-\frac{1}{\rho_g}\frac{\partial P_g}{\partial y}, \quad \ldots (44)$$

where ρ_g is the air density at the top of the transition layer, and P_g is the atmosphere pressure at same altitude. ρ_g is calculated using the ideal gas equation. The horizontal pressure gradients in Eqn. (44) are estimated by using the linear interpolation method as illustrated by the following steps. The pressure $P(x, y, z)$ can be interpolated from the three surrounding weather stations using the following relationship,

$$P(x,y,z)=\sum_{k=1}^{3}L_kP(x_k,y_k,z_k)$$

$$L_k=\frac{1}{D}(a_k+b_kx+c_ky)$$

$$D=\begin{bmatrix}1 & x_1 & y_1\\ 1 & x_2 & y_2\\ 1 & x_3 & y_3\end{bmatrix} \quad \begin{matrix}a_1=x_2y_3-x_3y_2, & b_1=y_2-y_3, & c_1=x_3-x_2\\ a_2=x_3y_1-x_1y_3, & b_2=y_3-y_1, & c_2=x_1-x_3\\ a_3=x_1y_2-x_2y_1, & b_3=y_1-y_2, & c_1=x_2-x_1\end{matrix} \quad \ldots (45)$$

where D is the determinant of the array, and L is the area of a sub-triangle that can be drawn from the location of a weather station inside the river basin and the locations of two reference weather stations that are located outside the river basin. The horizontal pressure gradients can be calculated by taking the derivatives of the pressure or,

$$\frac{\partial P(x,y,z)}{\partial x}=\sum_{k=1}^{3}\frac{\partial L_k}{\partial x}P(x_k,y_k,z_k),$$

$$\frac{\partial P(x,y,z)}{\partial y}=\sum_{k=1}^{3}\frac{\partial L_k}{\partial y}P(x_k,y_k,z_k)$$

$$\frac{\partial L_k}{\partial x}=\frac{b_k}{D}, \quad \frac{\partial L_k}{\partial y}=\frac{c_k}{D} \quad \ldots (46)$$

The components of the geostrophic velocity are calculated at deferent altitudes within the transition layer. The calculation stops when the divergence between successive geostrophic velocities is small. The analytical solution is given by,

$$u(z)=u_g\left[1-e^{\frac{-Z}{\Delta}}\cos\left(\frac{Z}{\Delta}\right)\right]$$

$$v(z)=u_ge^{\frac{-Z}{\Delta}}\sin\left(\frac{Z}{\Delta}\right) \quad \Delta=\sqrt{\frac{2K_E}{f}} \quad \ldots (47)$$

where z is the height above the ground surface.

The value of K_E can be estimated by substituting the measured wind velocity, which is taken form the weather stations inside the river basin at 10 m height, and apply the following formulas,

$$f=2\Omega\sin(\Phi_S)=8.365x10^{-5} \quad at\ Tsuchiyama(\Phi_S=35^\circ)$$

$$1-\frac{u(z)}{u_g}=e^{\frac{-Z}{\sqrt{2K_E/f}}}\cos\left(\frac{z}{\sqrt{2K_E/f}}\right)$$

$$z=10\Rightarrow\cos\left(\frac{z}{\sqrt{2K_E/f}}\right)\approx 1\Rightarrow\ln\left[1-\frac{u(z)}{u_g}\right]=\frac{-z}{\sqrt{2K_E^0/f}}$$

$$K_E^0=\frac{fz^2}{2\left[\ln\left(1-\frac{u(z)}{u_g}\right)\right]^2} \qquad K_{E(z=10)}^0=\frac{8.365\times10^{-5}\times(-10)^2}{2\left[\ln\left(1-\frac{u(10)}{u_g}\right)\right]^2}$$

$$\varepsilon=\frac{u(10)}{u_g}-e^{\frac{-10}{\sqrt{2K_E/8.365\times10^{-5}}}}\sin\left(\frac{10}{\sqrt{2K_E/8.365\times10^{-5}}}\right) \quad \ldots (48)$$

where ε is a very small number that approaches zero, and K^0_E is the constant exchange coefficient that is calculated by simplifying the equation of $u(z)$. The stopping criteria are; a very small ε, and the deference between K_E and K_{0E} is minimum.

WATER QUALITY MODELING

Necessity of Water Quality Analysis

The water related pollution sources are yearly increasing due to exploding urbanization and extensive use of detergents and chemicals in agricultural and industrial production. A reliable understanding of the chemical fate of pollutants is required for the environmental impact assessment. The simulation of surface runoff quality is based on assumptions related to pollutant accumulation and transport process. These assumptions are: (1) the spatial and temporal pollutant

concentration depends on the distributed runoff and the initial concentration of pollutant available for removal; (2) pollutant transformations due to chemical changes or biological degradation during the runoff process is considered, and (3) the amount of pollutants percolating into the soil by infiltration are significant. The distributed concentration of pollutant is estimated based on land use types and population in each grid.

Nonylphenol (NP) is selected as a case study in order to illustrate the methodology in this study, because it has been detected by many researchers in surfactant groundwater, sediment, aquatic organisms, wastewater effluent, air, and human food. (NP) differs from other persistence synthetic organic compounds such as: (PCBs), (DDT), and (PAHs) because it is not released directly into the environment, but it results from the anaerobic degradation of widely used nonionic surfactants, NPEO, which are neither toxic nor have an estrogenic effects, it is typically used in domestic liquid Landry detergents and used in cleaners (Porter *et al.*, 2001).

Pollutant Transport

The compartmental ("well-mixed" media) model of environmental fate and transport are used in order to describe the entry, movement, and spatial and temporal concentration of pollutants within the watershed. It is assumed each watershed consists of a number of well-mixed sub-compartments. Biotic and abiotic first order degradation processes have been considered; which are donated by K_i in each phase i. Advective and diffusive transfer between the phases are donated by U_{ik}, where the sequence i-k means the transfer from i phase to phase k. The following general form of the chemical balance equation, which takes into account all the degradations and interphase transfer processes in the compartments with volumes v_i and v_k, it considers each of the chemical species (x_i) in the model system,

$$\frac{dC_i^{x_i}(t)}{dt} = -K_i^{x_i}C_i^{x_i}(t) - \sum_k U_{ik}^{x_i}C_i^{x_i}(t) + \sum_k U_{ki}^{x_i}\frac{v_k}{v_i}C_k^{x_i}(t) + \sum_k \theta_i^{x_i x_2}K_i^{x_i}C_i^{x_i}(t) \quad \ldots (49)$$

where the first term on the right-hand side of Eqn. (49) represents degradation, the second term describes transfer between compartments, and the last term is the transfer form other compartments to the considered compartment.

Transformation Product of the Nonylphyenol Ethoxylate

The main source of the Nonylphyenol Ethoxylate (NPE) is the wastewater, which is released from wastewater treatment plants. Wastewater treatment can be techniques can be based on aerobic conditions, anaerobic conditions and combination of aerobic and anaerobic conditions.

Figure 3 shows the degradation of long-chain NPE during wastewater treatment. It was found that 45% of the NPE are still found in the secondary effluents and digested sewage. The concentration of NP form the wastewater treatment plant in the atmosphere is simulated using the Gaussian plume method and the generated wind filed. The spatial and temporal NP emissions rate is calculated based on the following assumptions:

- Emissions from the wastewater treatment plant into river are estimated by considering the number of sewers connections (population).
- Emissions from the wastewater treatment in the atmosphere are mixed completely with precipitation.
- The accumulated concentration of NP at each mesh is washed by runoff and a certain amount infiltrates into the unsaturated zone according to the distributed soil and land uses, and then ends in groundwater aquifer.
- Separated Sewer System (SSS) is assumed.
- The depth of sediment layer in river channel and paddy fields is assumed to be constant.

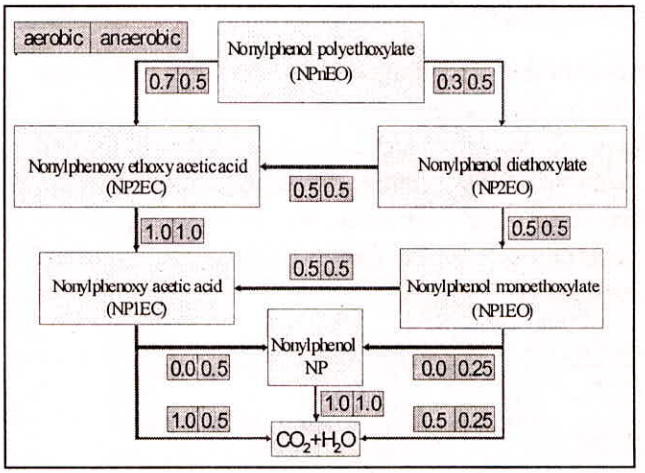

Fig. 3: Simplified transformation schemes of NPnEO in wastewater treatment plants and in natural environments

NP has been detected in atmospheric samples by many researchers, the air concentration of NP ranging from 2.2 to 70 ng/m^3. The volatilization should also be considered as a degradation mechanism when dealing with the environmental fate of NP, because of its moderate volatility (Henry's law constant ranges from 1.55×10^{-5} to 4×10^{-5} atm-m^3/mole) it enters the atmosphere from the aqueous phase. Gaussian plume model is used for calculating the spatial and temporal concentration of NP. The main assumption is that dispersion in the horizontal and vertical direction take the form of a normal Gaussian curve, and is given by,

$$C(x,y,z,t) = \frac{Q_{NP}(x,y,t)}{2\pi V \sigma_x \sigma_y} \exp\left[\frac{-y^2}{2\sigma_y^2}\right]$$

$$\left[\exp\left(\frac{-(z-H)^2}{2\sigma_z}\right) + \exp\left(\frac{-(z+H_e)^2}{2\sigma_z^2}\right)\right] \quad \ldots (50)$$

where, C is the spatial and temporal concentration of NP, QNP is the rate of NP emission, V is the wind speed, σ_y is the standard deviation in the y-direction, σ_z is the standard deviation in the z-direction, y is the distance along a horizontal axis perpendicular to the wind, z is the distance along the vertical axis, and H_e is the effective height of emission. The concentration along the ground, centerline, and with no plume rise is calculated by setting y, z and H_e to be 0.0.

APPLICATION OF HYDROBEAM INTO THE YASU RIVER BASIN

Simulation Results of Water Quantity

HydroBEAM is simulating the spatial and temporal water quantity and quality interactions in the atmosphere and in the ground. The simulated and observed snow depths are shown in Figure 4 at the Yasu River basin. The fluctuations are caused by the calibration of the model. Since the hydrological parameters of the distributed land uses and soils are varying for each grid, the calibration of the discharge at one station will not necessarily lead to good agreements between the observed and simulated values at other observation stations. The river discharge measurements at the Yasu River are performed daily. The daily measurements do not show the propagation of the kinematic wave from the upper catchments due to averaging of hourly readings. The simulated and observed daily discharges at Minakuchi station are shown in Figure 5.

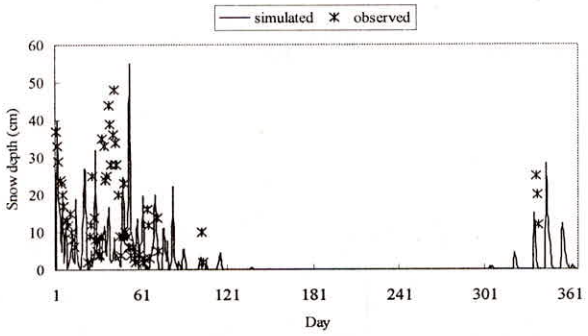

Fig. 4: Time series of the simulated and observed snow depths at the Yasu Dam, (1997/02/01, time: 00)

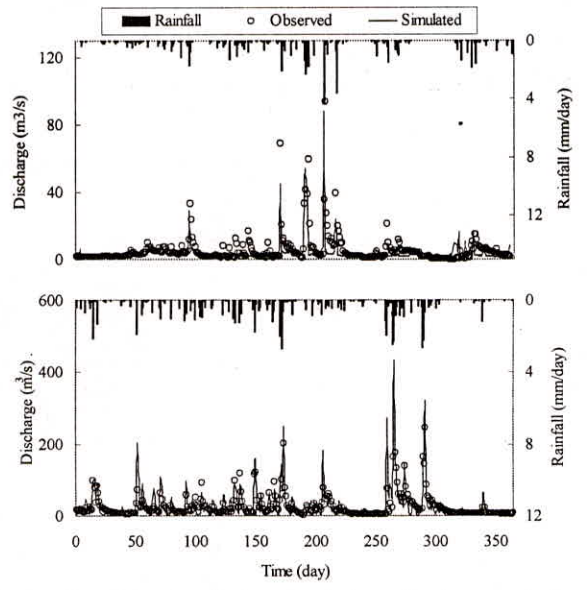

Fig. 5: Simulated and observed river discharges in lower Yasu River basin; upper chart: (1997), lower chart: (1998)

Figure 6 shows the plots of the flow hydrographs at various points along the river channel in the lower catchments, respectively. At the Yasu River basin the groundwater potential head value ranges from –40 to –100 m, the soil layer is divided into (100) divisions between the surface and the groundwater level. Then the soil moisture and the distribution of the potential head is simulated at every 10 sec, during this small time step the groundwater level is assumed to be steady and doesn't affected by the soil moisture.

At every large time step the groundwater level is updated in order to set the lower boundaries for the unsaturated flow model. Since the initial potential head for dry conditions is smaller than any of the distributed hydraulic conductivities, it is assumed that the soil will absorb a certain amount of the applied sources. The

distributed groundwater levels for upper and lower catchments are shown in Figure 7.

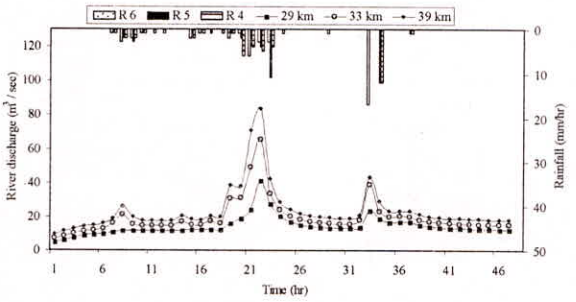

Fig. 6: Hourly river discharge sequences in lower catchments

Simulation Results of Atmosphere Quality

The generated wind is used with Gaussian plume model to calculate the distribution of NP that when emitted form a single point source located at Minaguchi. Since emission data was not it is approximated based in daily generation of wastewater. Figure 8 shows the spatial distribution of NP.

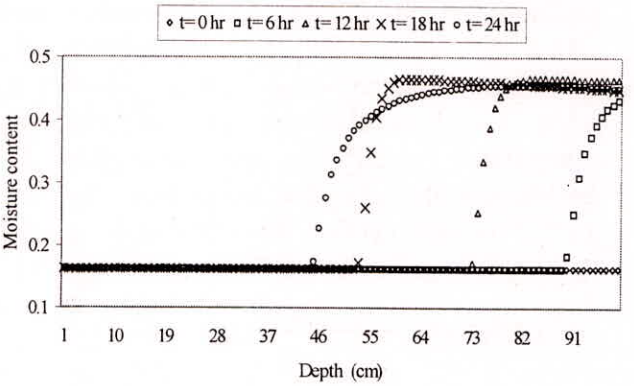

Fig. 7: Simulated groundwater level in the Yasu River basin

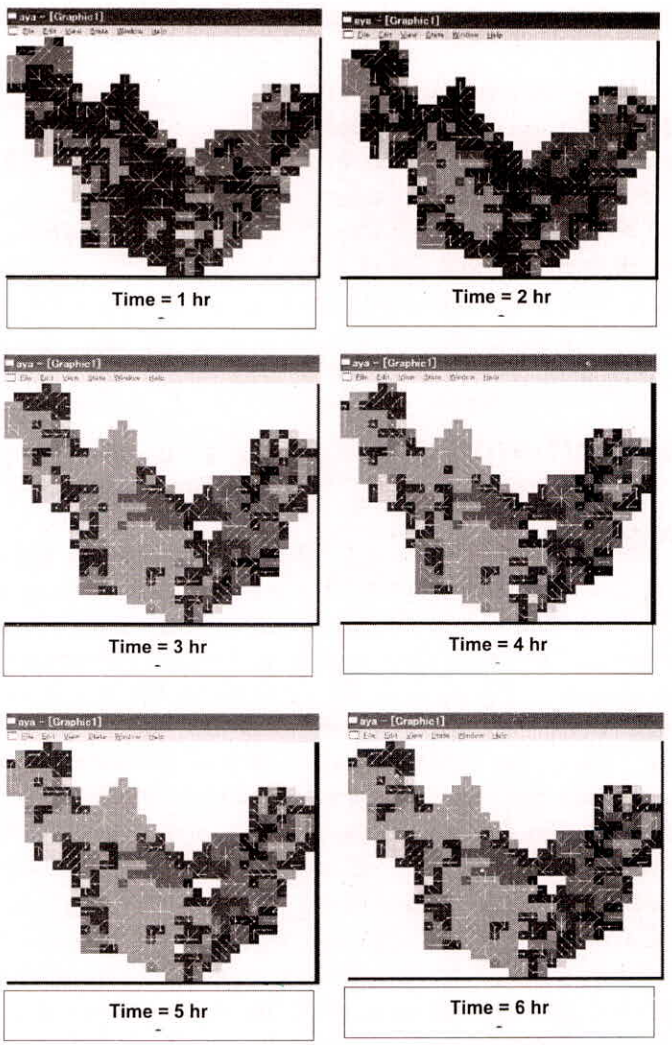

Fig. 8: Spatial and temporal distribution of NP and its concentrations that ranges form 90 ng/m^3 near the emission source and 2.2 ng/m^3 15 km far away

CONCLUSIONS

The main objective of this dissertation was to establish dynamically linked and physically based mathematical relationships with numerical approaches between distributed runoff models, groundwater and atmosphere models in order to simulate the hydrological interactions in the three zones. A general framework for the three dimensional hydrological modeling has been presented. The framework includes three main linked models; distributed rainfall-runoff model, groundwater flow model, and simplified atmosphere model. The importance of linking the three models for water quantity and quality has been illustrated and emphasized.

The mathematical formulations of the interactions in three zones using the dynamic linking have been achieved by using of the watershed characterization methodology.

The nourly records at few locations can be used to estimate the spatial and temporal ambient temperature, atmosphere pressure, and wind velocity in each grid. And then water quantity is simulated, and water quality can be simulated using the compartmental ("well-mixed" media) model. The developed HydroBEAM was applied for the case of the Yasu River basin. The spatial and temporal water quantity was presented and the simulations were compared with the observed data. The simulated groundwater levels and the river discharges showed good agreements with the corresponding observed values.

REFERENCES

Baker, D.L. (1995b). "Darcian weighted inter-block conductivity means for vertical unsaturated flow", *Groundwater*, Vol. 33, No. 3, 385–390.

Curtis, D.C. and Eagleson, P.S. (1982). "Constrained stochastic climate simulation", MIT Department of Civil Engineering, *Technical Report No. 274.*

Crawford, C.B. and Legget, R.F. (1957). "Ground temperature investigations in Canada", *Engineering Journal,* Vol. 40, No. 3, pp. 263–269.

FAO. (1998). "Crop evapotranspiration guidelines for computing crop water requirements", *Irrigation and drainage paper No. 56.*

Hiroh, A., Shioshige, K. and Ootaki, A. (1992). "Simulation of the plume model with the curved trajectory on the data of a diffusion experiment", School of Science and Engineering, Waseda University.

Idso, S.B. (1981). "A set of equations for full spectrum and 8–14 m and 10.5 um, Thermal radiation from cloudless skies", *Water Resources Res.*, Vol. 17(2), 295–304.

Jansson, P.E. (1991). "SOIL: simulation model for soil water movement and heat conditions", *Technical Report No. 165,* Swedish University of Agricultural Science, Department of Soil Science, 73.

Kojiri, T. (2000). "GIS-based environment model for water quantity and quality with river basin simulation", Annual DPRI, Kyoto University, Vol. 44, No. 1, 150–160.

Pielke, R.A. "Mesoscale Meteorological modeling", (1984), Academic Press, Orland.

Potter, T.L., Simmons, K., Wu J., Sanchez-Olvera, M., Kostecki, P. and Calabrese, E. (1999). "Static die-away of a Nonylphenol Ethoxylate surfactant in estuarine water samples", *Environ. Sci. Technol.*, Vol. 33, 113–118.

Richards, L.A. (1931). "Capillary conduction of liquids through porous media". *Physics 1*, 318–333.